JGR Planets

RESEARCH ARTICLE
10.1029/2021JE007152

Key Points:

- A detailed local study of a system of seven previously unknown palaeolakes near the dichotomy in western Arabia Terra, Mars
- High resolution topographic data aids in identification and characterization of palaeolakes and regional hydrological history
- Evidence for a prolonged history of fluvial and lacustrine processes, with palaeolakes fed by groundwater and surface accumulation

Correspondence to:
Z. I. Dickeson,
z.dickeson@nhm.ac.uk

Citation:
Dickeson, Z. I., Grindrod, P. M., Davis, J. M., Crawford, I., & Balme, M. (2022). Hydrological history of a palaeolake and valley system on the planetary dichotomy in Arabia Terra, Mars. *Journal of Geophysical Research: Planets*, *127*, e2021JE007152. https://doi.org/10.1029/2021JE007152

Received 7 FEB 2022
Accepted 12 NOV 2022

Author Contributions:
Conceptualization: Z. I. Dickeson
Investigation: Z. I. Dickeson
Methodology: Z. I. Dickeson
Project Administration: P. M. Grindrod
Supervision: P. M. Grindrod, J. M. Davis, I. Crawford, M. Balme
Writing – original draft: Z. I. Dickeson
Writing – review & editing: P. M. Grindrod, J. M. Davis, I. Crawford, M. Balme

Hydrological History of a Palaeolake and Valley System on the Planetary Dichotomy in Arabia Terra, Mars

Z. I. Dickeson[1,2], P. M. Grindrod[1], J. M. Davis[2], I. Crawford[2], and M. Balme[3]

[1]Department of Earth Sciences, Natural History Museum, London, UK, [2]Department of Earth and Planetary Sciences, Birkbeck College, University of London, London, UK, [3]School of Physical Sciences, The Open University, Milton Keynes, UK

Abstract Hundreds of ancient palaeolake basins have been identified and cataloged on Mars, indicating the distribution and availability of liquid water as well as sites of astrobiological potential. Palaeolakes are widely distributed across the Noachian aged terrains of the southern highlands, but Arabia Terra hosts few documented palaeolakes and even fewer examples of open-basin palaeolakes. Here we present a detailed topographic and geomorphological study of a previously unknown set of seven open-basin palaeolakes adjacent to the planetary dichotomy in western Arabia Terra. High resolution topographic data were used to aid identification and characterization of palaeolakes within subtle and irregular basins, revealing two palaeolake systems terminating at the dichotomy, including a ~160 km chain of six palaeolakes connected by short valley segments. Analysis and correlation of multiple, temporally distinct palaeolake fill levels within each palaeolake basin indicate a complex and prolonged hydrological history during the Noachian. Drainage catchments and collapse features place this system in the context of regional hydrology and the history of the planetary dichotomy, showing evidence for both groundwater sources and surface accumulation. Furthermore, the arrangement of large palaeolakes fed by far smaller palaeolakes, indicates a consistent flow of water through the system, buffered by reservoirs, rather than a catastrophic overflow of lakes cascading down through the system.

Plain Language Summary Evidence for hundreds of ancient lakes has been found on Mars, but these features are not distributed uniformly across the surface, and the vast majority of evidence for past lakes and valleys on Mars is found within the ancient southern highlands of the planet. In this work we describe a newly discovered system of ancient lakes and river valleys which end at the geologically important boundary between the southern highlands and northern lowlands. Global catalogs of ancient lakes on Mars have generally relied on relatively low-resolution imagery and topography, but for the small area covered in this study we were able to utilize high-resolution imagery, and produce new high-resolution topographic maps. This detailed approach allowed identification of multiple past water levels within each lake, and paired with an analysis of other features formed by lakes and rivers, we reconstructed a history of lake filling, drainage, and eventual decline and disappearance. These reconstructions reveal that drainage through the system was sustained over a prolonged period, rather than a single catastrophic event. Discovery and description of similar systems across Mars with these techniques will aid in placing further constraints on the history of liquid water and habitable environments on Mars.

1. Introduction

The widespread occurrence of liquid water on ancient Mars is supported by evidence for hundreds of palaeolakes within the Noachian aged (>3.7 Ga) southern highlands (Cabrol & Grin, 1999, 2001; Fassett & Head, 2008b; Fawdon et al., 2021; Goudge et al., 2012, 2015, 2016, 2021; Irwin III et al., 2005). The global characterization and distribution of palaeolakes has helped to constrain past climatic and hydrological conditions on Mars (Kite, 2019; Milliken et al., 2010; Wilson et al., 2016), and to identify possible past habitable environments (Fairén et al., 2010). Studies of individual palaeolake systems have contributed to our understanding of regional hydrological histories, and although palaeolake ages generally coincide with the end-Noachian peak in global fluvial activity, many examples indicate multiple episodes of locally or regionally controlled lacustrine activity rather than a global hydrological system stable over geological timescales (Di Achille et al., 2009; Goudge & Fassett, 2018; Mangold & Ansan, 2006; Salese et al., 2016; Wilson et al., 2016). The continued incorporation of detailed palaeolake studies into regional and global contexts, including relationships to fluvial, groundwater and possible ocean systems, will provide a broader understanding of hydrology on Mars.

Martian palaeolakes are identified primarily upon morphological relationships between topographic basins and fluvial valley networks, and categorized as either open-basin or closed-basin. Open-basin palaeolakes are defined by outflow valleys, indicating a fill level sufficient to breach and overflow the basin (Cabrol and Grin, 1999, 2001; Fassett & Head, 2008b). Open-basin palaeolakes are therefore the strongest evidence for standing bodies of water and are commonly associated with regionally extensive drainage systems and branching valley networks (Goudge et al., 2016), and indicate a greater supply and duration of liquid water than a similarly sized closed-basin palaeolake which never filled to the point of overflow. Conversely, closed-basin lakes exhibit only inlet valleys, and are typically fed by isolated, shallowly incised valleys (Goudge et al., 2015, 2016). Most palaeolakes currently described on Mars occur within conspicuous impact craters, while a minority have been reported in tectonically controlled basins (Mangold & Ansan, 2006), inter-crater basins bounded by the upraised rims and ejecta of multiple impact craters (Goudge & Fassett, 2018), and other basins of undefined origin (Irwin III et al., 2002, 2004).

The distribution of globally cataloged Martian palaeolakes (Fassett & Head, 2008b; Goudge et al., 2016) approximately correlates to that of valley networks (Alemanno et al., 2018; Hynek et al., 2010). Palaeolakes are thus almost entirely limited to the southern highlands, and many palaeolake and valley systems terminate at the edge of the northern lowlands (Figure 1). The processes leading to the formation and present morphology of the planetary dichotomy are not well understood (Watters et al., 2007), but the dichotomy may represent the margins of an ancient, hemisphere spanning ocean (Clifford & Parker, 2001; Di Achille & Hynek, 2010; Duran et al., 2019; Parker et al., 1986). Regardless of the processes involved, the dichotomy appears to mark a distinct hydrological boundary, and analysis of the fluvial and lacustrine systems terminating here is important to understanding the geological history of this planet encircling feature (Dickeson & Davis, 2020).

Here, we identify and describe a group of previously undocumented palaeolakes situated adjacent to the planetary dichotomy in Arabia Terra. Making use of high-resolution digital elevation models (DEMs), we analyze the topographic relationships between multiple equipotential palaeolake levels, sedimentary fans, longitudinal valley profiles, and associated geological features. Our objective is to produce a detailed history of lacustrine and fluvial processes in the area, and place these processes within the context of regional hydrology. The fluvial and lacustrine systems which intersect or terminate at the dichotomy in this area present an additional opportunity to investigate the origin and modification of the dichotomy scarp, as well as questions regarding the existence of lowland water bodies (Di Achille & Hynek, 2010).

1.1. Study Area in Western Arabia Terra

This study covers an area of ~22,000 km^2 near the planetary dichotomy in western Arabia Terra, approximately 920 km NNE of Oxia Planum and 370 km NE of the terminus of Mawrth Vallis. The area was identified whist browsing orbital imagery for possible deltas along the dichotomy scarp, and chosen for a focused study upon discovery of a large delta fed by a highland valley system exhibiting evidence of lacustrine processes. Arabia Terra exhibits a paucity of open-basin palaeolakes (Fassett & Head, 2008b; Goudge et al., 2012) and valley networks (Alemanno et al., 2018; Carr, 1995; Hynek et al., 2010), but an abundance of inverted channel systems indicative of a depositional fluvial setting (Davis et al., 2016, 2019; Dickson et al., 2020; Williams et al., 2018). In addition, the lowest areas of western Arabia Terra, near the dichotomy, are suggested as sites of significant groundwater upwelling (Andrews-Hanna et al., 2010; Fassett & Head, 2008b; Salese et al., 2019), and numerous northern ocean palaeoshorelines have been mapped along this section of the dichotomy (Dickeson & Davis, 2020).

The Arabia Terra region of the southern highlands is predominantly Noachian in age and is bounded to the north and west by the planetary dichotomy, and sits at a markedly lower elevation than the majority of the southern highlands. Further setting the region in contrast to the wider highlands is evidence of significant resurfacing and exhumation (Schmidt et al., 2021, 2022), with erosion depths on the scale of 10^2–10^3 m (Evans et al., 2010; Zabrusky et al., 2012). The topographic consequences of these processes are most visible at the edge of the lowlands, where deposition and erosion of a mantling layer up to 60 m in thickness may influence the morphology of the dichotomy scarp (Fassett and Head III, 2007), as well as the distribution and morphology of mesas within lowland terrains (McNeil et al., 2021).

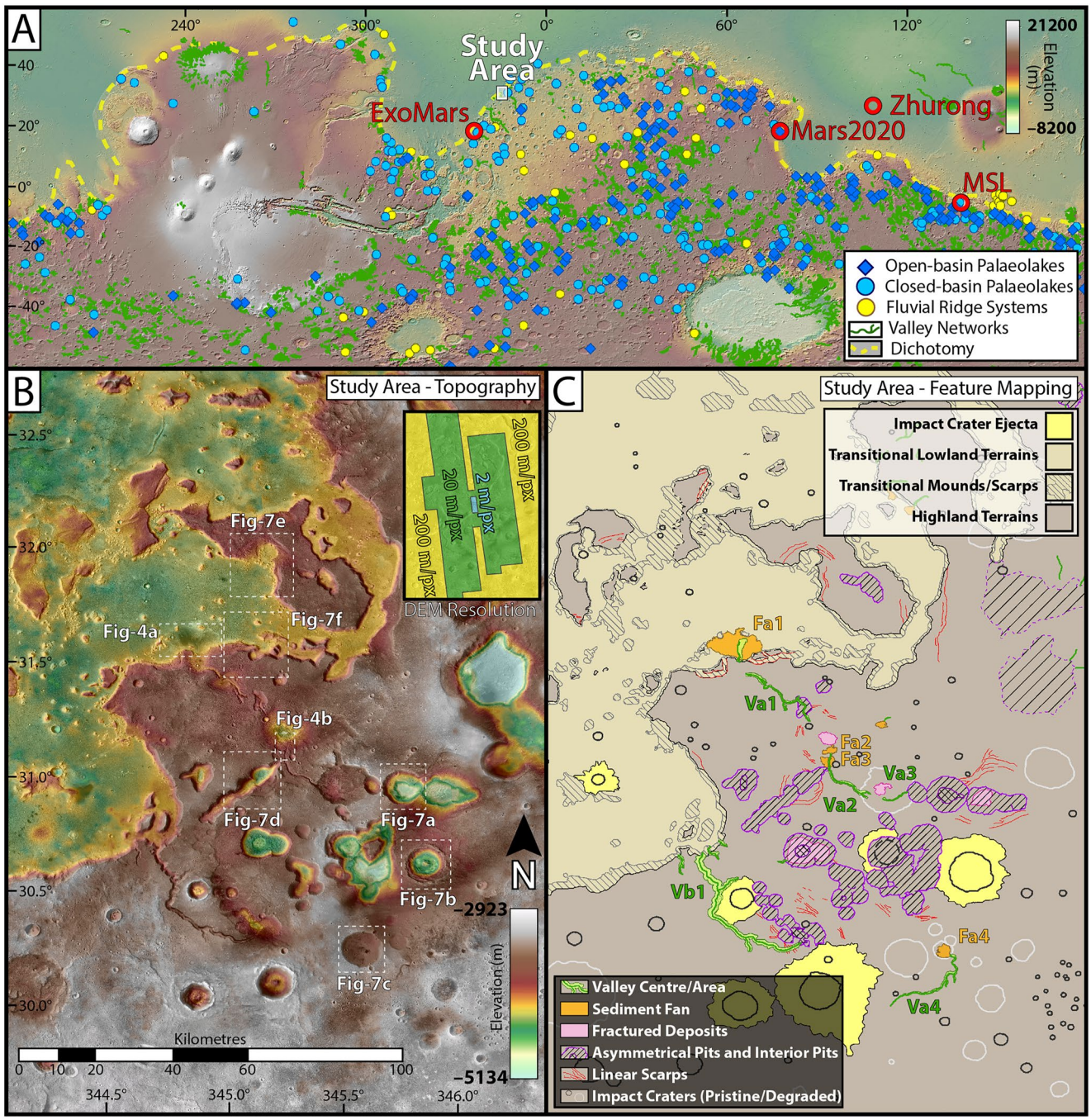

Figure 1. (a) Global topographic map (top) showing the study area in relation to globally cataloged open-basin (dark blue diamonds (Goudge et al., 2012)) and closed-basin (light blue circles (Goudge et al., 2015)) palaeolakes, valley networks (green lines (Alemanno et al., 2018)), and fluvial ridge systems (yellow circles (Dickson et al., 2020)), an approximation of the planetary dichotomy (yellow dashed line), and the planned (ExoMars) and presently active (MSL, Zhurong & Mars 2020) rover landing sites. (b) Topographic and CTX mosaic map of the study area and digital elevation model (DEM) resolutions (inset: mosaic including HRSC, CTX, and HiRISE DEMs). (c) Morphological features of interest on a high resolution remapping of highland (brown) and lowland (tan) terrains.

Our study focuses on an area of the dichotomy marking the topographic and geological boundary between the middle Noachian highland terrains (mNh), and the Noachian-Hesperian transitional lowland terrains (HNt (Tanaka et al., 2014)). In this study, the geological units have been remapped at CTX resolution (Figure 1c), with the contact tracing the steep scarp of the dichotomy and including large flat topped mesas to the east of the dichotomy as a part of the highland terrains (Tanaka et al., 2003, 2014).

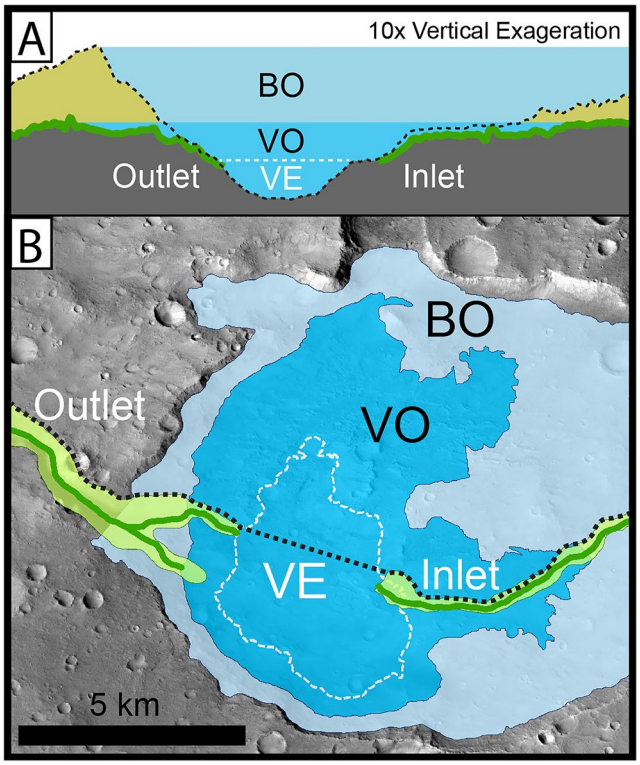

Figure 2. Method used to identify palaeolake basins, and equipotential surfaces. (a) Cross-section of topographic basin exhibiting an inlet and outlet valley, with two palaeolake levels defined by elevations of the outlet valley: basin overflow (BO), defined as the highest elevation contour within the basin with a single opening at the outlet valley; and valley overflow (VO), defined as the highest closed contour intersecting the outlet valley. The valley extremity (VE) elevation, defined as the lowest contour intersected by the outlet valley is also shown, but is not a clear indication of palaeolake level. (b) Map-view showing the two palaeolake extents (BO, light blue; VO, blue), describing equipotential surfaces defined by the elevations observed at the outlet valley.

2. Data and Methods

Geomorphological feature mapping was carried out using imaging data from NASA's Context Camera (CTX; ~6 m/pixel (Malin et al., 2007)), with additional images from the High Resolution Imaging Science Experiment (HiRISE; 0.25–0.50 m/pixel (McEwen et al., 2007)), and daytime infra-red images from the Thermal Emission Imaging System (THEMIS; 100 m/pixel; thermal (Christensen et al., 2004)).

High-resolution topographic data was used in the identification and characterization of landforms, and to define the possible hydrological relationships between mapped landforms. Topographic data was created from mosaicked CTX (20 m/pixel) and HiRISE (2 m/pixel) DEMs with approximate vertical precisions of <8 and <1 m, respectively (Kirk et al., 2008), and supplemented with High Resolution Stereo Camera (HRSC; 150–200 m/pixel (Neukum & Jaumann, 2004)) DEMs and Mars Orbital Laser Altimeter (MOLA; 456 m/pixel (Smith et al., 2001)) topography data. DEMs were produced from stereo CTX and HiRISE imagery and MOLA shot heights using ISIS3 and SOCETSET software and the USGS workflow (Kirk et al., 2008).

2.1. Hydrological Analysis

Mapping and analysis were carried out using ESRI ArcMap software, with "Spatial Analyst" and "Hydrology" toolboxes used to identify equipotential surfaces, basins, and drainage catchments. Palaeolake basins were defined by equipotential surfaces within closed topographic basins at the elevations of outlet valley heads (Fassett & Head, 2008b; Goudge et al., 2012). This was achieved by generating contours at 10 m intervals, and selecting the highest closed contour at each valley head, thus defining an equipotential surface nearly overflowing the basin through the outlet valley which we refer to as the "valley overflow (VO)" level (Figure 2). We expanded on this logic to identify an additional palaeolake level at a higher equipotential surface within each basin, identified as the highest contour with a single opening at the outlet valley which we refer to as the "basin overflow (BO)" level. A lower elevation was also defined by the lowest closed contour at the valley head which we refer to as the "valley extremity (VE)" level, although this observation was not in itself interpreted as an equipotential surface (Figure 2).

Drainage catchments were produced using the ArcMap "Hydrology" toolbox on a mosaicked topographic data set of CTX and MOLA DEMs encompassing the wider highlands region. The "Fill" tool was used to generate a topography with no local sinks. This preparatory step negates the influence of small sinks and noise in the topographic data to produce an idealized drainage catchment, which is necessarily exaggerated as all sinks are filled regardless of depth, age, or origin. This filled topography becomes the basis for production of flow direction and flow accumulation rasters, with pour points manually selected at locations of significant flow accumulation. Drainage catchments were then calculated using the "Watershed" tool, which outputs the total upland area which would contribute surface runoff for each pour point.

3. Observations and Results

In this section, we describe the morphological features mapped in this work (Figure 1c). (Section 3.1) Valleys and (Section 3.2) sediment fans represent the best evidence for liquid water in the study area, and are analyzed in detail to identify and (Section 3.3) define palaeolake basins and levels. Hydrological sources and sinks are analyzed in relation to highland drainage catchments, (Section 3.4) and basins within the lowlands, respectively.

(Section 3.5) The final section describes conspicuous scarp and pit features observed within the study area, and the relationships of these features to mapped valleys and palaeolakes.

3.1. Fluvial Valleys

Incised valleys were identified and mapped on CTX imagery, with valley centerlines following the lowest elevation along the valley floor, and valley sides mapped to ascertain width and incision depth. Our analysis focused on the five longest valleys in the study area, ranging from 7.5 to 47 km in length, and numbered from the dichotomy in order of increasing mean valley elevation (Figure 3). A few short (<6.6 km) tributary valleys are also present, but do not represent significant branching networks. The valleys are typically "V" shaped in profile, with narrow, flat floors dominated by aeolian bedforms and lacking visible interior channels. The heads of all major valleys begin within closed basins in the highland terrains. The two longest and deepest valleys (Va1 and Vb1) terminate at the dichotomy, while the others (Va2–Va4) terminate within highland closed basins.

All valleys begin with a short section of negative slope in comparison to the overall trend of the valley, meaning the elevation of the valley head is 30–260 m lower than the maximum elevation of the valley floor. In addition, longitudinal profiles of the two valleys which terminate at the dichotomy reveal the lower reaches of Va1 to be comparatively low slope compared to the upper reaches, and the lower reaches of Vb1 to be higher slope than the upper reaches, with the transition between the two sections of Vb1 marked by a knickpoint coincident with the intersection of a tributary (Figure 3d).

In close proximity to Vb1, are four short but deeply incised valleys. Three of these valleys terminate at the dichotomy, and unlike Vb1, appear incised into the dichotomy scarp (Figure 3d). The fourth valley nearby terminates within an asymmetrical pit in the Noachian highland terrains.

3.2. Sediment Fans

Broad fan shaped features (Fa1–Fa4) with areal extents of 5.1–69.7 km^2 are observed with apexes extending from the termini of three valleys (Va1, Va2, Va4). They have lobate, distal edges marked by steep scarps and relief of ∼1–100 m above surrounding terrains, typical traits of Gilbert type deltas. Fan surfaces are heavily degraded and cratered, but are in general flat, with low and consistent downward slopes from apex to distal edge (Figure 3).

The largest fan (Fa1) is situated at the dichotomy at the terminus of valley Va1, with distal lobes which appear to deflect around raised mounds and mesas (Figure 4a), and although the contact relationship is unclear, the fan appears to lie above transitional lowland terrains (Tanaka et al., 2014). The fan surface is marked by numerous channels and hosts a high concentration of aeolian bedforms compared to surrounding terrains, suggesting the fan comprises fine grained, sand-grade material sourcing the aeolian bedforms. Exposed layering is ∼1 m thick, sub-horizontal and parallel.

Two fans at the terminus of valley Va2 are situated at different elevations, with the upper fan (Fa3) incised by the valley which terminates at the lower fan (Fa2) (Figure 4b). The upper fan (Fa3) has a sharply-defined lobate form with steep distal edges, and sub-horizontal, parallel, layering of ∼1 m thick. The lower fan (Fa2) is heavily degraded, with poorly-defined edges, and an irregular surface topography. The internal structure of Fa2 appears to be complex, with layering ∼1–10 m thick, steeply dipping and possibly crosscutting with stacked lobes and channels also visible (Figure 4d). Some areas are densely covered by aeolian bedforms, again suggesting a fine grained sedimentary material composes the fan.

The fan (Fa4) at the terminus of valley Va4 nearly covers the floor of an eroded impact crater (Figure 3c). The fan surface is heavily cratered, but has a general sub-horizontal upper surface, with steep distal edges, several shallow channels incised into it, and ∼1 m thick, sub-horizontal, parallel bedding exposed in the walls of impact craters.

3.3. Open Basin Palaeolakes

Seven possible palaeolake basins were identified where closed topographic basins are situated at the heads of valleys, or transected by valleys. These were numbered in order of increasing elevation of the outlet valley from the dichotomy as follows; three (La1–La3) associated with valley Va1, one (La4) with valley Va2, one (La5)

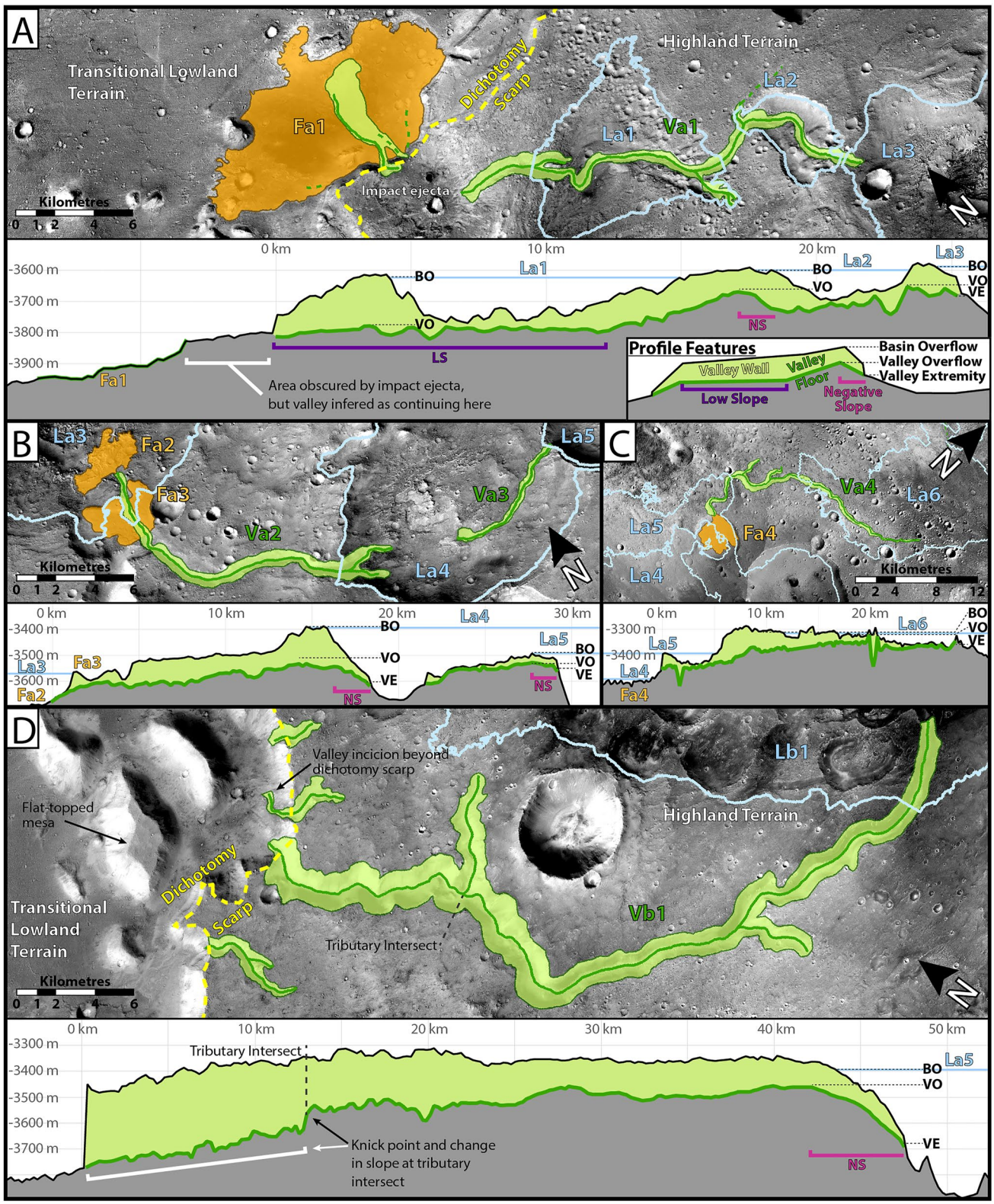

Figure 3. Detail images and longitudinal valley profiles for the five major valleys (dark green valley center and light green area between valley sides), with relationships to sedimentary fans (orange areas), the dichotomy (yellow dashed line), and maximum possible palaeolake extents (light blue lines). Slope features indicated on valley profiles include: negative slope heads (NS, pink), and low slope lower reaches (LS, purple), with three outlet valley elevations marked where valleys transect or begin within topographic basins at: headward valley extremity (VE), valley overflow at the maximum valley floor elevation (VO), and basin overflow at the maximum valley side elevation (BO) (CTX imagery, with profiles derived from CTX DEMs).

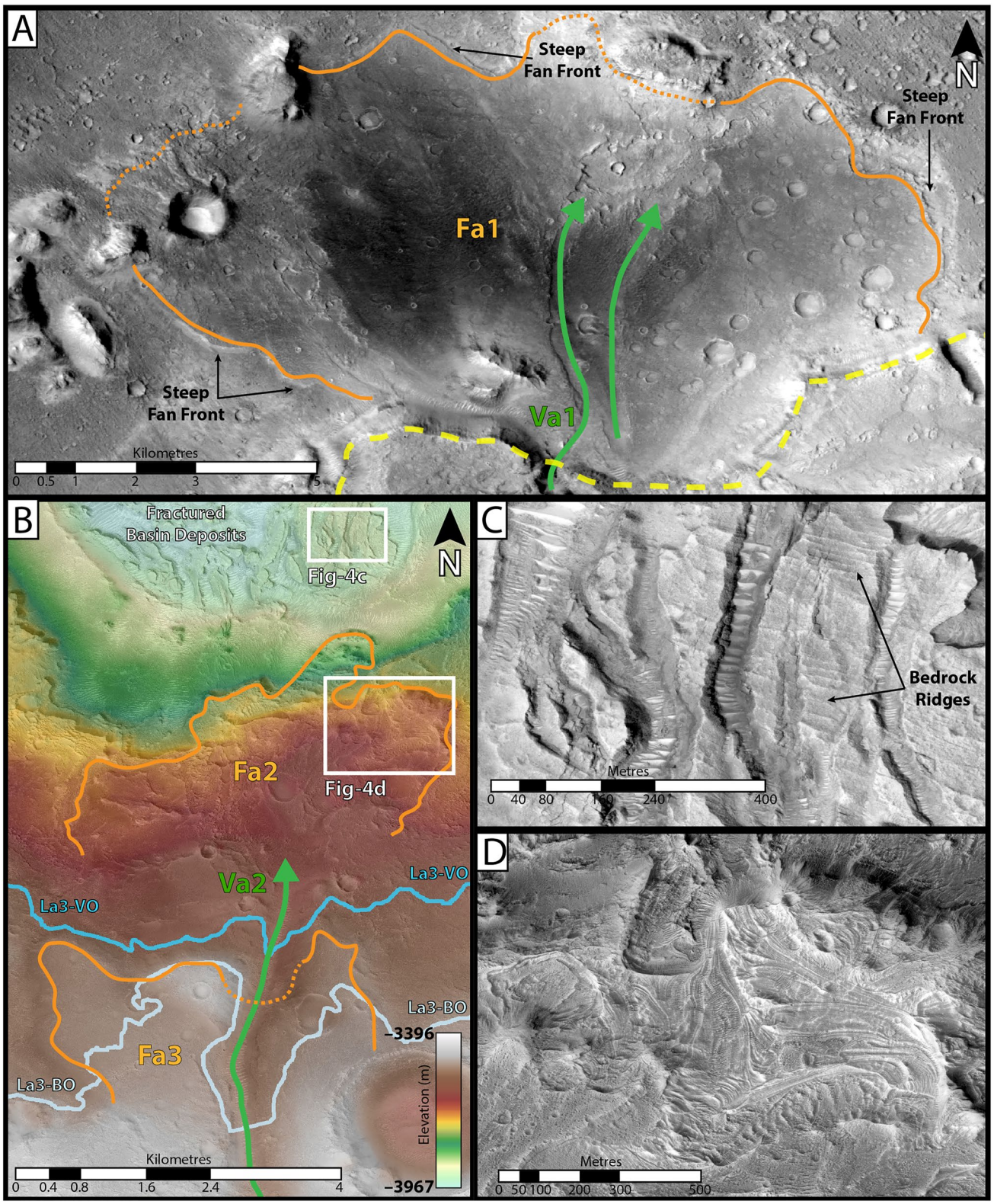

Figure 4.

with valley Va3, one (La6) with valley Va4, and one (Lb1) with valley Vb1 (Figure 5). Outlet valley elevations (Figure 3) for VO and BO were recorded, with each level interpreted and mapped as representing a possible equipotential surface and palaeolake fill level. Palaeolake volumes were calculated for each of the fill levels based on the current topography (Table 1).

The BO level represents the highest possible palaeolake level within each basin, based on a fill and spill model in which a basin filled with water and then overflowed on a topography existing before full incision of an outlet valley. However, if an alternate process such as sapping erosion or mass wastage controlled initiation of outlet erosion then the actual maximum palaeolake level may have been lower. The VO level represents the lowest palaeolake level maintaining drainage through the outlet valley, based on overflow out of a water filled basin along the fully incised outflow valley floor. The VE level marks the lowest elevation of incision of the outlet valley, below the palaeolake surface, and is likely the result of sub-aqueous erosion caused by high flow rates at the initiation of drainage and lake breaching (Fassett & Goudge, 2021; Goudge, Fassett, and Mohrig, 2019; Marra et al., 2014). However, in palaeolake basins La3 and La4 the VE level correlates well with the elevation of inlet valley terminations, and may indicate the surface level within closed-basin palaeolakes existing after (Table 1).

Locations and elevation of valley terminations and possible deltas were also considered as supporting evidence of palaeolake levels, although in isolation these features do not conclusively indicate a standing body of water (Table 1). As observed above, two valley terminations (Va2 and Va3) correlate closely to VE levels (La3, +3 m; La4, −7 m), and although valley Va4 is poorly correlated to a BO level (La5, +45 m) the elevation (−3,445 m) falls between the BO levels of La4 (−3,390 m) and La5 (−3,490 m). The mean elevations of two possible deltas (Fa2 and Fa4) correlate well to BO levels (La3, −4 m; La5, −7 m), and that of fan Fa3 is situated somewhat below the VE level (La3, −29 m).

The irregular palaeolake geometries exhibited in this study suggest a variety of basin origins, with the majority of palaeolakes (La1, La3, La5, La6, and Lb1) hosted within relatively shallow, irregular shaped basins without conspicuous edges. This is in contrast to globally cataloged martian palaeolakes which are often hosted within conspicuous impact craters (Cabrol & Grin, 1999; Goudge et al., 2015). In our study, only one palaeolake is hosted within an impact crater (La4), and another is within a deep asymmetrical pit (La2) of uncertain origin.

Basin floor deposits with a fractured appearance are observed within deeper areas of palaeolake basins La3, La4, La5 and Lb1 (Figure 1c). These deposits are characterized by raised blocks (∼150–500 m) separated by steep-sided, flat-floored fissures, and deposits within palaeolake basin La3 are shown in Figure 4b. The sides of fractured blocks reveal fine (∼1–10 m) layering, and the surfaces of some blocks display a corrugated appearance, with the orientation of minor fractures apparently influenced by the orientation of corrugations in the bedrock surface (Figure 4c).

3.4. Highland Drainage Catchments and Lowland Sinks

Drainage catchments were calculated on a topography with all local sinks filled to determine the maximum extent of highland areas where accumulated surface water could drain into the northern lowlands (Figure 6). Calculations of this kind do not consider topographic modification postdating fluvial processes, such as large recent craters, and are thus order of magnitude estimates of the true palaeo-catchment. Two drainage end points were chosen where valleys Va1 and Vb1 terminate at the dichotomy, describing two drainage basins, "A" and "B" respectively, separated by a drainage divide. Drainage catchment "A" has an area of 69,404 km^2 and extends south from the apex of possible delta Fa1 nearly to Mawrth Vallis. In contrast, the area of drainage catchment "B" is an order of magnitude smaller at 3,393 km^2, and only extends a maximum of ∼65 km from palaeolake Lb1. Most of the palaeolakes identified in this work fall within catchment "A" (La1–La6), and only one within catchment "B" (Lb1). The drainage divide runs between the narrow (<2 km) raised area separating palaeolakes La5 and Lb1, the two largest in the study area, indicating no surface connection between these two water bodies. Drainage

Figure 4. Detailed images of sediment fans and basin floor deposits in the study. (a) Situated on the dichotomy, at the termination of valley Va1, Fa1 is the largest sediment fan in the study. The fan margin (orange line) describes the steep front of the fan above the surrounding lowland terrains, and the different surface within the fan area (CTX image). (b) The outlines of sediment fans Fa2 and Fa3 (orange lines) are shown here approximately correlating respectively to the VO (blue contour) and BO (light blue contour) levels of palaeolake La3, and in relation to fractured basin floor deposits (HiRISE image with HiRISE DEM). (c) A detail of basin floor deposits highlights fine layering, and the corrugated surface typical of these deposits across the study area (HiRISE image). (d) A detail of the complex bedding exposed in the heavily weathered surface of sediment fan Fa2 (HiRISE image).

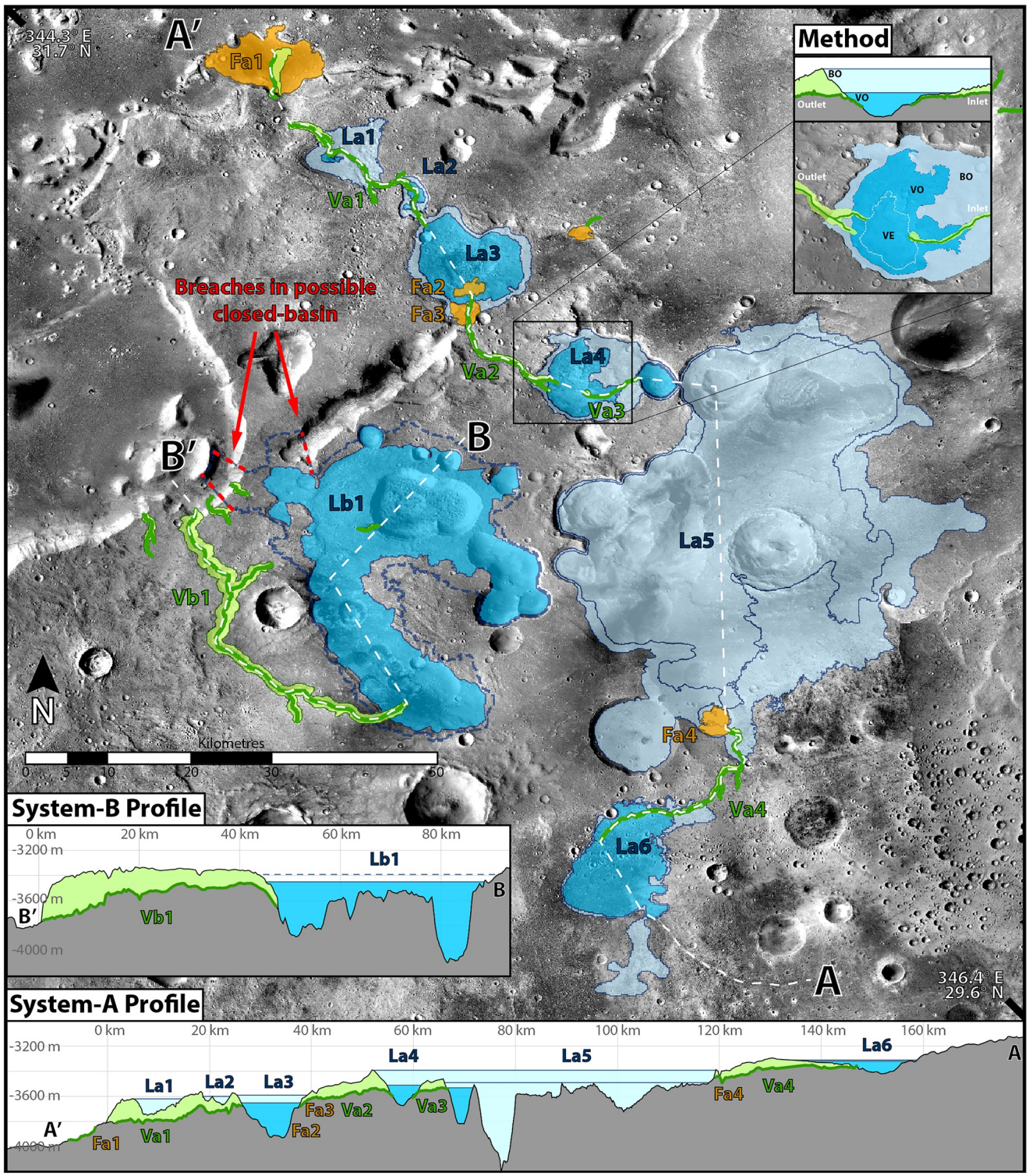

Figure 5. Palaeolake extents and lake/valley system profiles based on outlet valley elevations: basin overflow (BO; light blue), and valley overflow (VO; mid blue). System-A profile displays a close correlation of palaeolake surfaces with inlet valleys and sediment fans. System-B map and profile include an approximate basin overflow level (dashed blue line), defining a nearly closed contour with the narrow areas open to the lowlands (red dashed lines). Both profiles displayed at the same scale and vertical exaggeration (CTX imagery and HRSC/CTX DEM mosaic).

Table 1
Palaeolake Surface Elevations and Dimensions for Each Outlet-Defined Fill Level (BO, VO) Within Each of the Seven Palaeolake Basins (La1–La6, Lb1)

			Correlated fill level elevations		Palaeolake dimensions				Drainage catchment	
Palaeolake	Fill level	Surface elevation (m)	Inlet valley term (m)	Mean sediment fan (m)	Area (km^2)	Volume (km^3)	Mean depth (V/A) (m)	Max depth (m)	Sub-basin (km^2)	Total basin (km^2)
La1	BO	−3,620	–	–	55	4.08	76	200	498	69,347
	VO	−3,770	–	–	2.6	0.06	14	50	–	–
La2	BO	−3,600	–	–	14	0.79	58	140	87	68,849
	VO	−3,660	–	–	6.1	0.17	28	80	–	–
La3	BO	−3,590	–	−3,594	135	18.5	138	370	971	68,762
	VO	−3,650	–	–	98	11.5	117	310	–	–
	VE	−3,680	−3,677	−3,709	83	8.82	107	280	–	–
La4	BO	−3,390	–	–	1,691	456	271	1,110	252	67,791
	VO	−3,510	–	–	52	3.45	67	170	–	–
	VE	−3,600	−3,607	–	15	0.63	41	80	–	–
La5	BO	−3,490	−3,445	−3,483	1,062	311	300	1,010	12,955	67,539
	VO	−3,530	–	–	13	2.05	163	320	–	–
La6	BO	−3,310	–	–	188	7.85	42	180	54,584	54,584
	VO	−3,320	–	–	125	6.15	40	170	–	–
Lb1	BO	−3,390	–	–	803	154	192	840	3,303	–
	VO	−3,450	–	–	586	106	183	780	–	–

Note. Drainage catchment areas are shown for individual palaeolake basins and cumulatively for palaeolakes in the system-A chain.

sub-basins were calculated for each of the identified palaeolakes, and cumulative catchment areas calculated with higher sub-basins contributing to progressively lower sub-basins (Table 1).

Both drainage systems "A" and "B" terminate at the planetary dichotomy, at elevations defining a basin encompassing the entire northern lowlands. Locally however, the area surrounding the valley termini defines a nearly closed basin with only limited lower elevation gaps between flat topped mesas and mounds (Figure 6). If the terminal fan (Fa1) associated with this valley (Va1) is indeed a delta, it would indicate a standing body of water at the time of formation. The contour at the mean elevation of fan Fa1 is −3,940 m, defining a nearly endorheic basin with a total perimeter of ∼408 km, which is closed along 99% of its length, with the maximum single gap being 2.7 km. The maximum elevation of fan Fa1 is −3,778 m, defining a wider basin with a perimeter of ∼499 km, which is still closed along 87% of its length, with the widest single gap being 15 km. However, we note that characterizing this fan as a delta as opposed to an alluvial fan formed in a dry basin is not possible with the diagnostic observations presented in this work, and that further investigation may be required to distinguish between these possibilities.

3.5. Scarp and Pit Features

In addition to the observed fluvial and lacustrine landforms in the study area, a number of conspicuous scarp and pit features were mapped and described as part of this study. Many of these features are in close proximity to palaeolake basins, and in some cases define of influence the mapped extents of palaeolakes. In this section we describe the morphology of pits and scarps, and their apparent relationships to mapped palaeolake basins, as well as to the morphology of the regionally important dichotomy scarp. Three types of pit morphologies were identified in this work: two with established formation processes and timings, (a) pristine impact craters, (b) degraded impact craters; and a third type of uncertain origin, (c) asymmetrical pits.

Pristine impact craters (Figure 7b) exhibit raised rims, steep interior sides, a uniform depth to diameter ratio, and often have raised central peaks and ejecta blankets. These craters are thought to postdate the palaeolakes, but only the two largest palaeolakes (La5 and Lb1) are superposed by large pristine impact craters or their ejecta, and they

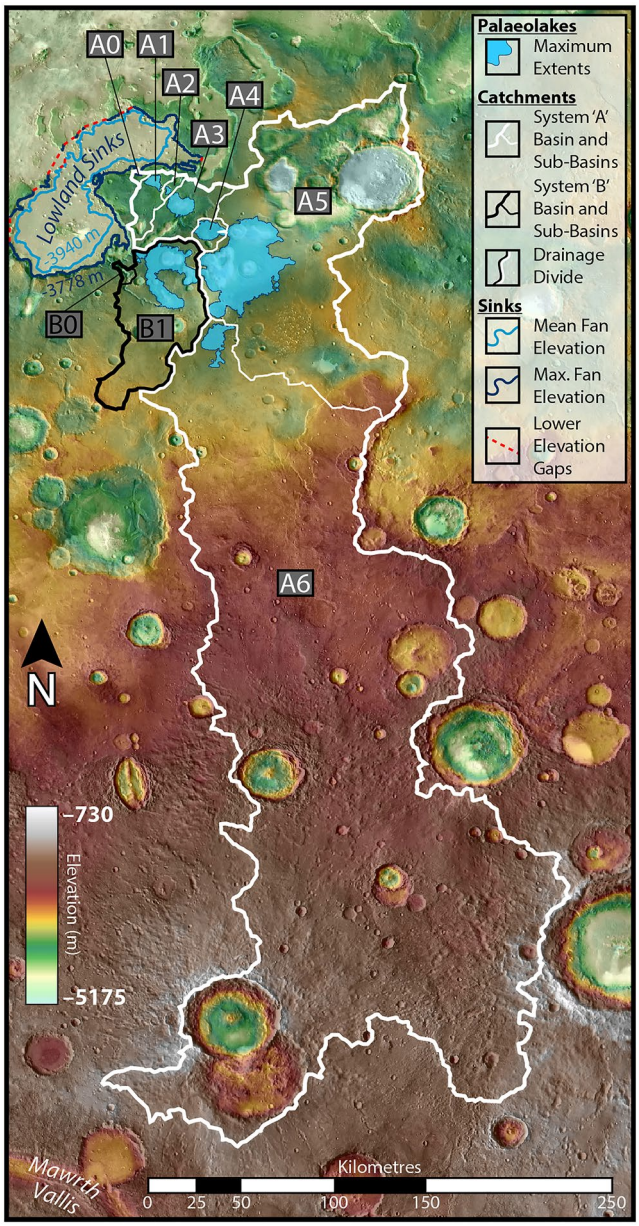

Figure 6. Highland drainage catchments for palaeolake systems "A" (white borders) and "B" (black borders) terminating at the dichotomy, showing numbered sub-basins (thinner white and black borders respectively) for each individual palaeolake (light blue areas). Possible fill levels within lowland sinks are shown for the mean (light blue dashed line) and maximum (dark blue dashed line) elevations of sediment fan Fa1, indicating basins nearly closed to the northern lowlands with only narrow gaps between flat topped mesas (red dashed lines) (background is THEMIS daytime mosaic overlain on MOLA hillshade).

do not appear to greatly influence measurements of palaeolake dimensions. Filled, eroded, or otherwise degraded impact craters (Figure 7c) are typically shallow and flat floored, with no uniform depth to diameter ratio. Palaeolake basin La4 is situated entirely within a degraded crater, and the southern edge of palaeolake basin La5 is partially defined by overlapping degraded craters.

Asymmetrical pits (Figures 7a and 7d) are limited to the Noachian highland terrains and concentrated near the mapped palaeolakes. Small asymmetrical pits are bowl-shaped in profile and circular or semi-circular in plan-view. Larger examples appear to be composed of conjoined smaller pits, and are typically asymmetrical with cuspate or scalloped edges and narrow curvilinear interior ridges (Figure 7d). Pit edges are sharply-defined, without raised rims, and have relatively consistent depths with no uniform depth to diameter ratio. Some asymmetrical pits also host secondary interior pits which are morphologically similar to the primary pits. Palaeolake La2 is situated completely within an asymmetrical pit, and although limited lengths of other palaeolake edges (La4, La5, Lb1) are defined by asymmetrical pits, the majority are situated fully within palaeolake basins La5 and Lb1. Asymmetrical pits appear to be one of the youngest features in the study area, forming abrupt, steep, sharp edges where they intersect degraded impact craters, valleys (Va3), and the ejecta of pristine impact craters (Figure 1c). Given the significant depth of these features, the calculated water-holding volumes in basins with asymmetrical pits (La4, La5, and Lb1) may be gross overestimates if the pits formed subsequent to palaeolakes.

The dichotomy scarp marks the sharp contrast between the highland and lowland terrains (Figure 7f), and has a prominence of up to ~600 m in the study area, reducing to ~300 and ~100 m at the terminus of valleys Vb1 and Va1 respectively. In profile, the dichotomy scarp is very steep, and in planform displays a cuspate geometry similar to the asymmetrical pits, and the scarps surrounding large flat-topped mesas (Figure 7e). The morphological similarity between these landforms may indicate a common formational origin for all three features.

The dichotomy scarp where intersected by valley Va1 (−3,900 m) is low and gently sloping, and sediment fan Fa1 appears to have formed over lowland deposits (Figure 4a). In contrast, valley Vb1 (−3,800 m) terminates abruptly at the dichotomy with no sediment fan and without extending beyond the high steep scarp in this area (Figure 3d). These relationships suggest that in the area of valley Va1 the dichotomy scarp predates fluvial activity, but that in the area of valley Vb1, alteration (e.g., erosional retreat) of the dichotomy scarp has occurred which postdates fluvial activity.

Smaller linear scarps with heights of ~1–100 m are observed within the Noachian highland terrains, commonly as pairs and sets arranged in parallel, with depressed troughs between inward dropping scarps (e.g., similar to a graben structure), or stepwise with scarps set progressively lower, and are consistent with troughs formed as a result of lateral spreading. Linear scarps are concentrated near, and subparallel to, the margins of asymmetrical pits (Figure 7d), the dichotomy scarp (Figure 7f), and the edges of large flat-topped mesas (Figure 7e), and were likely formed at the same time.

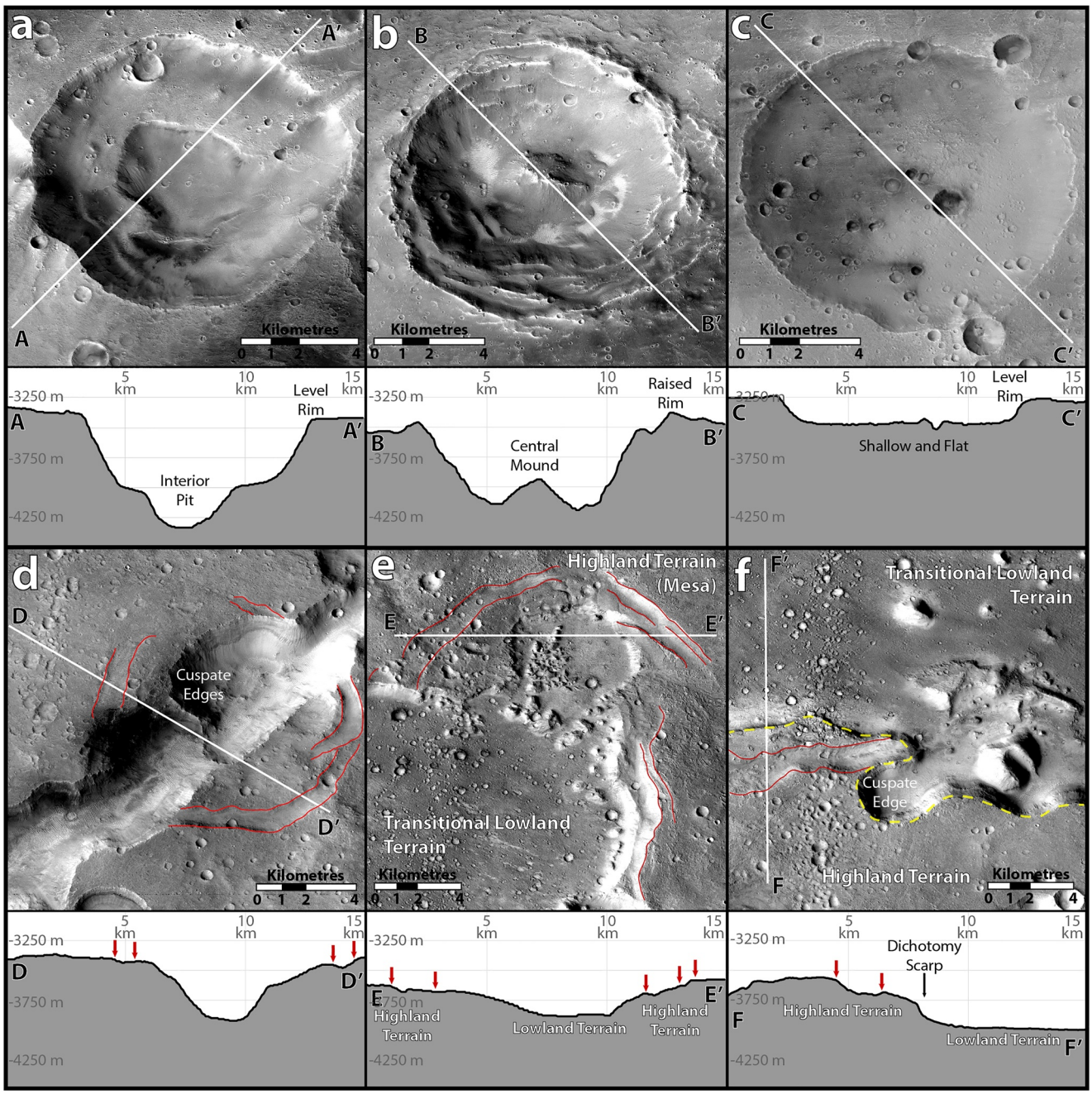

Figure 7. Morphological pit and scarp landforms which influence the topography of the study area are displayed here in plan-view and profile. (a) Asymmetrical pits display no raised rim, steep sides, and often a secondary interior pit, and although this example is circular in planform these features are distinct from: (b) pristine impact craters displaying raised rims, steep sides, and central mound, and (c) degraded impact craters displaying slight raised rims and shallow flat floors., (d) More commonly observed are asymmetrical pits with irregular shapes and cuspate edges, apparently formed from coalesced circular and sub-circular pits, and often surrounded by linear scarps (red lines and arrows). The planforms and profiles of asymmetrical pits are similar to the edges of (e) large flat-topped mesas, again with linear scarps (red arrows), and (f) also to the dichotomy scarp (yellow dashed line), also shown in association with linear scarps. North is up in all images. Profiles for a-e shown at the same vertical exaggeration. All images from CTX, and profiles generated on CTX DEMs.

4. Discussion

4.1. Palaeolake Overflow and Valley Incision

Defining a sequence of events leading to the overflow of palaeolake basins and incision of outlet valleys was a central goal of this study, and laid out here are the observations guiding these interpretations. Outlet valley

defined BO and VO levels are interpreted as marking temporally distinct water levels at the initiation and cessation of drainage out of each palaeolake basin, with an interceding period of falling palaeolake levels driven by outlet valley incision.

Basin overflow levels represent the highest possible water levels and extents of palaeolakes at the initiation of BO immediately prior to outlet valley incision, and have been calculated similarly to other studies (Goudge & Fassett, 2018; Salese et al., 2020). Basin overflow levels within catchment "A" (La1–La6) all define basins with the lowest basin margin coincident with an outflow valley (Figure 5), supporting a model of surface flow and outlet valley incision initiated as higher basins filled and spilled over these saddles to fill lower basins. However, sapping erosion and upstream propagation of valley heads from lower to higher basins likely contributed to valley incision, and in turn may have played a role in the initiation of breaching in some basins.

In contrast, the BO level in palaeolake basin Lb1 does not describe a closed basin, and the contour at this elevation (−3,360 m) is open to the northern lowlands and inconsistent with a palaeolake on the current topography. In this case, it appears that the present topography is not representative of the topography which existed at the time of the palaeolake, and as a maximum palaeolake level cannot be determined with certainty, and we considered the −3,390 m contour to be a conservative approximation of palaeolake level prior to outlet valley incision. This level defines a nearly closed basin only broken at the dichotomy scarp and by asymmetrical pits which appear to postdate palaeolakes and valleys.

As incision of outlet valleys progressively lowered the elevation of valley heads, this in turn lowered palaeolake water levels, reduced palaeolake extents, and allowed inlet valleys to incise further and lower into palaeolake basins (Figure 5). Valley incision may have progressed gradually as a result of continuous drainage during some periods, but was likely also punctuated by multiple discrete overspill events as evinced by the subaqueous erosion observed at outlet valley heads. However, the arrangement of large palaeolakes in the middle of the system (La5) fed by smaller upstream palaeolakes (La6), suggests a constant flow through the system rather than the filling and breach of a single large source basin.

As the system matured, outlet valley incision continued to reduce palaeolake extents throughout the system until the input flux of water to each lake was no longer sufficient to significantly erode the valleys. The VO levels therefore represent the open-basin palaeolakes at the cessation of outlet valley incision, although overspill and drainage could have continued for some time without contributing to incision. When inlet water flux was eventually overtaken by the rate of water loss through infiltration and evaporation, then overflow ceased and these basins would have become closed-basin lakes.

4.2. Processes at the Planetary Dichotomy

Valley terminations and deltas are often interpreted as representing the margin of a hemisphere spanning ocean on Mars when studied globally (ocean surface level −2,540 m (Di Achille & Hynek, 2010)), and locally (ocean surface level, −2,500 m (Fawdon et al., 2018)), and within Arabia Terra potential shorelines closely follow the dichotomy (Carr & Head, 2003; Clifford & Parker, 2001; Webb, 2004). However, topographic analysis of deltas in some regions indicate a number of lowland palaeolakes or small seas adjacent to the dichotomy, rather than the margin of a hemisphere spanning ocean (García-Arnay & Gutiérrez, 2020; Rivera-Hernández & Palucis, 2019). Significant changes in the morphology, elevation, and position of the dichotomy since the Noachian therefore have important implications for the mapping of lowland waterbodies adjacent to the dichotomy.

The morphological characteristics shared by the dichotomy scarp, mesa scarps, and the sides of asymmetrical pits (Figures 7d–7f) suggest a common origin, consistent with collapse and erosional retreat postdating fluvial and lacustrine activity. With similar processes implicated in the formation of mesas in the Oxia Planum area to the southeast of this study (McNeil et al., 2021). Significant collapse and erosional retreat along the dichotomy and within asymmetrical pits would explain the lack of a sediment fan or clear termination where valley Vb1 intersects the dichotomy, and would account for the existence of a previously closed basin for palaeolake Lb1 in the highlands.

Situated at the dichotomy, sediment fan Fa1 (−3,940 m), along with the termination (−3,815 m) and low slope lower reaches (−3,791 m) of valley Va1 constitute possible water levels within the northern lowlands (Duran et al., 2019). On the current topography these elevations would indicate a water body filling the entire northern

lowlands, but given evidence of collapse and erosional retreat along the edge of flat-topped mesas we instead propose that these levels indicate a palaeolake limited to a local lowland basin which was once closed (Figure 6). Our interpretation is that the both basins of both Lb1 and the lowland basin at Fa1 represent ancient palaeolakes which existed within closed basins, which were later destroyed by terrain collapse and erosional retreat. These examples highlight the challenges of martian hydrology being necessarily reliant on current topographic data, and the importance of observing evidence of major changes in topography.

Valley Vb1 displays a pronounced knickpoint corresponding to the intersection of a tributary valley (Figure 3), may indicate a significant lowering of base level within the northern lowlands basin, and more recent drainage forming the knickpoint and tributary. Similar knickpoints elsewhere on Mars have been interpreted as representing multiple episodes of fluvial activity and/or changes in base level (Duran et al., 2019; Goudge & Fassett, 2018).

4.3. Regional Hydrology and Martian Palaeolakes

Global palaeolake catalogs have so far identified only one open-basin palaeolake in western Arabia Terra (Fassett & Head, 2008b; Goudge et al., 2012), but local studies to the north and south of our study have identified additional examples (Fawdon et al., 2021; Wilson et al., 2016). The seven open-basin palaeolakes in this work are therefore significant in further characterizing the style, distribution, and frequency of lacustrine processes in the region, and add to the broader understanding of lacustrine systems on Mars.

The palaeolakes and valleys discussed in this work are situated within Noachian highland terrains (Tanaka et al., 2014), but this only affords an upper limit to their age. Determination of absolute ages for martian valley networks is difficult, and although a method for buffered crater counting has been successful in dating large valley networks (Fassett & Head, 2008a), the relatively short valleys (<47 km) in our study and preclude this as an option. Some of the valleys (Va2—Va4) and sediment fans (Fa4) clearly overly degraded impact craters, and although valley Vb1 appears to be either incised through or partially covered by the ejecta of a ∼5 km impact crater there are no unambiguous relationships between fluvial features and large pristine impact craters (Figure 1c). The approximate age of valleys, sediment fans and palaeolakes is therefore presumed as matching the Noachian peak in fluvial activity, postdating ancient degraded impact craters and predating pristine impact craters.

The peak in fluvial and lacustrine processes on Mars is generally agreed to have occurred during the Noachian to early Hesperian (Fassett & Head, 2008b; Goudge et al., 2016; Hoke et al., 2011; Howard et al., 2005; Irwin III et al., 2005; Kite, 2019), and some studies suggest palaeolakes were also active as late as the middle Amazonian (Wilson et al., 2016). One global study (Goudge et al., 2016) associates palaeolakes fed by extensive valley networks with an early period of formation prior to 3.7 Ga, and those fed by limited valleys with a later period of reduced hydrological activity during the Hesperian or Amazonian (<3.7 Ga). The palaeolakes in our study are difficult to categorize by these criteria, as they constitute a long chain of palaeolakes, yet are only connected by short, non-branching valleys. However, the greater supply and duration of liquid water required to fill open-basin palaeolakes, and the evidence supporting continuous flow through the system rather than a single catastrophic overflow, leads us to conclude that the palaeolake systems described in this work fit with the period of palaeolake activity prior to 3.7 Ga.

To sustain drainage through the system would have required a sufficiently warm and dense atmosphere to support liquid water, as well as a steady or repeated flux of water from precipitation or groundwater. A high ratio of palaeolake volume to catchment area ($V/A_{\text{Catchment}} > 15$) has been highlighted as an indication of filling dominated by groundwater rather than surface runoff, but only for palaeolakes not fed by other palaeolakes as part of a chain (Fassett & Head, 2008b). In our study a comparison is therefore only useful for palaeolakes Lb1 and La6 which are not fed by higher palaeolakes, and La5 which is only fed by a much smaller palaeolake (La6). Of these three palaeolakes, only Lb1 ($V/A_{\text{Catchment}} = 47$) displays a volume to catchment relationship indicative of groundwater as the dominant water source. While values for palaeolakes La5 ($V/A_{\text{Catchment}} = 4.6$) and La6 ($V/A_{\text{Catchment}} < 1$) support filling dominated by surface runoff from the substantially sized drainage catchment. Furthermore, palaeolakes Lb1 and La6 do not exhibit inlet valleys, and although this could be considered a further indication of filling by groundwater, it is possible that small inlets have been obscured or destroyed by subsequent processes.

Western Arabia Terra has been identified as a region of significant groundwater upwelling, particularly in areas adjacent to the dichotomy (Andrews-Hanna et al., 2010), and this process was probably important in filling

palaeolakes across the region (Fassett & Head, 2008b). Overflow of the palaeolakes in our study appears to have been primarily driven by surface drainage through the system, although it is possible that upwelling groundwater played a role in the original filling of these basins, with earlier palaeolakes existing as unconnected, closed-basin palaeolakes, only requiring minimal additional input to become sufficiently full to breach and drain.

The palaeolakes in this study are slightly smaller and shallower than the mean of globally cataloged of open-basin palaeolakes, but are well within the global range (Fassett & Head, 2008b). However, the majority of globally cataloged palaeolakes are hosted within conspicuous, steep-sided impact craters, whilst the population presented in this study are mostly hosted within subtle, irregular shaped basins without clearly defined edges. The limited availability and coverage of high-resolution data and the time required by this approach preclude a similarly detailed catalog of the entire highlands, but the findings of this study suggest that many more small extent, shallow depth, and subtle basin palaeolakes remain as yet unidentified. Alternatively, the detailed approach to analyzing multiple palaeolake levels presented in this study could be applied to palaeolake chains and systems already identified in global catalogs. Presenting an opportunity to derive further findings from existing data sets, and to contrast regional differences in palaeolake processes.

Fractured basin floor deposits are a feature common to many martian palaeolakes, including within the deepest palaeolake basins in an area to the north of our study (Wilson et al., 2016), with larger scale fractured floor deposits found in association with many other palaeolakes on Mars (Goudge et al., 2012). In Xanthe Terra, to the south of our study, these features are interpreted as having formed by rapid discharge and eventual groundwater depletion within closed palaeolake basins (Sato et al., 2010). Additionally, the ridged surfaces of some fractured floor deposits in our study appear analogous to the "washboard" terrains observed in Gale crater, where they are interpreted as aeolian dunes preserved beneath closed-basin palaeolake deposits (Favaro et al., 2021; Milliken et al., 2014). Finely bedded palaeolake deposits on Earth are often excellent records of paleoclimate, and are important settings for the concentration and preservation of organic material. Therefore, palaeolake deposits identified in this study present opportunities for orbital and surface based palaeo-climate and astrobiology studies, particularly where palaeolake deposits are exposed, such as where fracture in palaeolake La3 (Figures 4b and 4c), or incised by later fluvial erosion in palaeolake La1 (Figure 3a).

4.4. Local Hydrological and Geological Evolution

The identification of multiple palaeolake fill levels and varied morphological features in this work allows a reconstruction of the sequence of hydrological and geological processes leading to the observed palaeolakes and valleys, and although this history may be specific to the study area, it is likely to be partially representative of other palaeolakes observed in Arabia Terra. The precise mechanism initiating drainage of each palaeolake, and the order in which palaeolakes breached is difficult to ascertain, but groundwater fed closed-basin lakes could have existed in some or all of the basins before water flux was sufficient to initiate overflow, and although palaeolake overflow was eventually simultaneous throughout the system, initial breaching didn't necessarily progress from the top of the system downwards.

Palaeolake basin La6 is the only basin that shows evidence consistent with filling by surface accumulation without input from other palaeolakes, and is the highest basin in the area. The strong correlation between inlet and outlet valleys indicates that all the other palaeolakes (La1–La5), other than Lb1, were fed by inlet drainage ultimately originating from palaeolake La6. The fact that the volume of palaeolake La6 is so much smaller than lakes further down the system indicates that there was consistent flow through the system buffered by basin reservoirs, rather than a single filling and spilling event from top to bottom.

In system "A", a continuous chain of valleys and lakes drained water and sediment from the highlands to the lowlands, with palaeolakes cascading down through the system from basin La6, draining through valley Va4 to form sediment fan Fa4 and fill basin La4, draining through valley Va3 to form sediment fan Fa3 and fill basin La3, and then draining through valley Va1 (Figure 8e). Valley Va1 was originally three short isolated sections, with the first draining from La3 to fill basin La2, a second section draining La2 to fill basin La1, and a third section draining La1 and terminating at the dichotomy to form sediment fan Fa1. Higher up the system, the highest level of palaeolake La4 defined a very large palaeolake, with an outlet at valley Va2 matching the elevation of the inlet at valley Va4, and thus submerged the area that would later include palaeolake La5 and valley Va3 (Figure 8e).

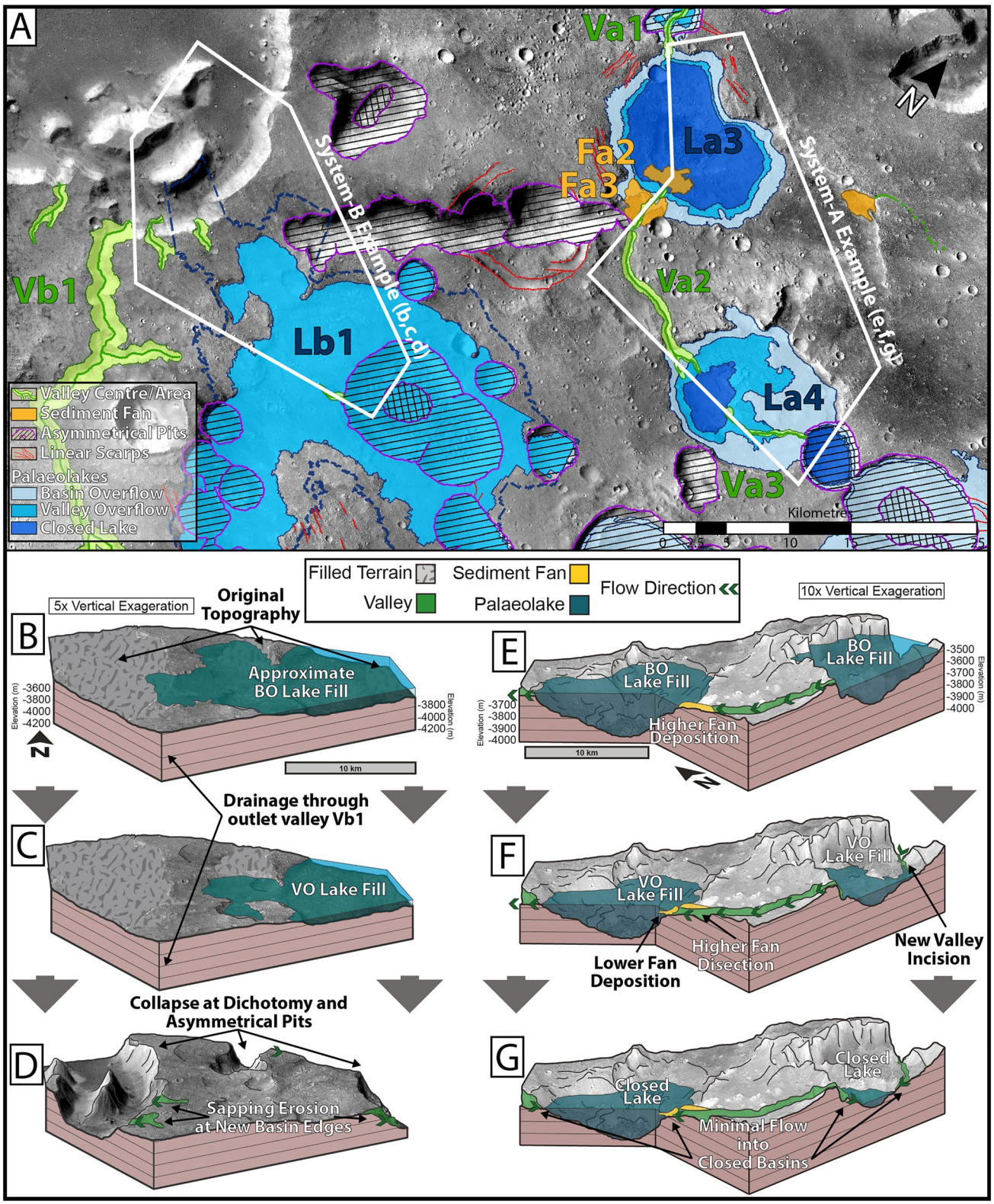

Figure 8.

In system "B", the limited drainage catchment and lack of inlet valleys suggest that basin Lb1 was filled by groundwater, and then drained through valley Vb1 to debouch into the lowlands (Figure 8b). The close proximity and correlated elevations of BO levels in La4 and Lb1 could also indicate groundwater communication between the two systems, with Lb1 partially fed by groundwater from the more extensive system "A." Significant groundwater flow in this area may also be supported by the later collapse of these areas, as suggested by the high concentration of asymmetrical pits between these palaeolakes.

Continued drainage through both systems led to progressively lower palaeolake levels caused by outlet valley incision lowering the elevation of the outlet spillway (Figures 8c and 8f). Significant outlet valley incision resulted in complete drainage of the palaeolakes in basins La1 and La2, allowing inlet valleys to incise the previously submerged lake floors to become one continuous valley (Va1). Incision of valley Va1 also caused water level to fall in basin La3, allowing inlet valley Va2 to incise down and through sediment fan Fa3, with the apex of a new sediment fan (Fa2) forming basinward at the new termination of valley Va2 (Figure 8f). Incision of valley Va2 caused a water level fall and significant reduction in lake extent within palaeolake La4, with the new smaller basin fed by a newly formed valley (Va3) draining from palaeolake La5 and incising across the previously submerged palaeolake floor. The late exposure of Va3 and sections of Va1 after being submerged would also explain the relatively shallow incision depth of these valleys.

At the cessation of palaeolake overflow and drainage, palaeolakes were filled to just below the VO level, and closed basins or ephemeral palaeolakes likely within some basins (La3–La6, Lb1) (Figures 8d and 8g). At some point after drainage through the palaeolake systems had ceased, collapse within highland terrains formed asymmetrical pits and modified the scarps of the dichotomy and the margins of flat topped mesas (Figure 8d). The resulting topography no longer reflected some original palaeolake volumes, and left gaps to the lowlands in the previously closed basin of Lb1 and a possible closed basin in the lowlands.

5. Conclusions

High resolution CTX imagery and DEMs facilitated the discovery and characterization of this palaeolake system, and allowed for precise calculations of palaeolake fill levels and drainage catchments. The identification of temporally distinct palaeolake fill levels linked to different outlet valley elevations was key to understanding changes is palaeolake levels and valley incision over time, and allowed fully drained palaeolake basins to be identified. Additional analysis of longitudinal valley profiles and possible deltas strengthens the evidence for these basins having hosted lakes, and provides insight into the hydrological evolution of the area.

Significantly, these palaeolakes indicate a combination of groundwater sources and surface accumulation, supported by a climate sufficiently warm and stable for prolonged fluvial and lacustrine processes during the Noachian. The discovery of finely bedded lake deposits laid down during this potentially habitable period, which are incised though by subsequent valleys, presents an ideal site for future palaeo-climatic and astrobiological exploration.

That such a complex yet localized system has not been included in previous catalogs suggests that many other hitherto unrecognized palaeolakes may exist on Mars, and are likely to be revealed with the increased use of high resolution images and topography. Compared to crater-hosted palaeolakes which are typically deep and exhibit clearly defined edges, palaeolakes of the type described here display more subtle topographic profiles, and are likely to be underrepresented in palaeolake catalogs. Undertaking similar detailed studies on the hundreds of palaeolakes already identified in global catalogs, has the additional potential to greatly expand our knowledge of water sources, comparative regional hydrology, and further characterize the past climate of Mars.

Figure 8. (a) Representative areas of system "A" including palaeolake basins La3 and La4; and system "B" including palaeolake basin Lb1 and the dichotomy scarp, and chronologies of fluvial and lacustrine processes in system "A" (e–g) and system "B" (b–d). The top diagrams (b and e) show the highest palaeolake fill levels (BO) at the initiation of palaeolake drainage, (e) with the formation of fan Fa3 at the end of valley Va2, (b) and an approximate topography with asymmetrical pits and the dichotomy scarp filled. The middle diagrams (c and f) show reduced palaeolake levels (VO) resulting from outlet valley incision while drainage out of the basins continued. (f) Fan Fa3 was incised through by valley Va2 to form the new lower fan Fa2, and lake level lowered within basin La4 so that valley Va3 began to incise across the former lake floor. The bottom diagrams (d and g) show the lowest palaeolake levels (VE), likely fed by ground water or minimal surface accumulation, (d) and the current topography resulting from the formation of asymmetrical pits and the dichotomy scarp (CTX imagery on CTX DEM topography).

Data Availability Statement

Primary image and topographic data used in this research can be accessed on the Mars Orbital Data Explorer of the Planetary Data System (PDS) (https://ode.rsl.wustl.edu/mars/) for: CTX (Malin et al., 2007), HiRISE (McEwen et al., 2007), and MOLA (Smith et al., 2001) data. A mosaic of the CTX DEMs produced for this work can be accessed on FigShare (Dickeson, 2022) (https://doi.org/10.6084/m9.figshare.19071560.v1). Geospatial calculations and mapping were carried out with ESRI ArcMap software (v.10.3.1), including the "3D Analyst" and "Spatial Analyst" extensions (https://www.esri.com/en-us/arcgis/products/arcgis-desktop/overview).

Acknowledgments
The authors would like to thank A. Garcia-Arnay and T. Goudge for insightful and constructive reviews which greatly improved the manuscript. Funding for this project and ZID was provided by the UK Science and Technology Facilities Council Grant STFC-1967420. MRB was supported by UK Space Agency Grants (ST/T002913/1, ST/V001965/1, ST/R001413/1), PMG was also supported by the UK Space Agency (ST/R002827/1, ST/R002355/1, and ST/W002744/1), and JMD gratefully acknowledges UK SA support (ST/R002355/1; ST/V002678/1; ST/W002566/1).

References

Alemanno, G., Orofino, V., & Mancarella, F. (2018). Global map of Martian fluvial systems: Age and total eroded volume estimations. *Earth and Space Science*, *5*(10), 560–577. https://doi.org/10.1029/2018ea000362

Andrews-Hanna, J. C., Zuber, M. T., Arvidson, R. E., & Wiseman, S. M. (2010). Early Mars hydrology: Meridiani playa deposits and the sedimentary record of Arabia Terra. *Journal of Geophysical Research*, *115*(Jun), E06002. https://doi.org/10.1029/2009je003485

Cabrol, N. A., & Grin, E. A. (1999). Distribution, classification, and ages of Martian impact crater lakes. *Icarus*, *142*(1), 160–172. https://doi.org/10.1006/icar.1999.6191

Cabrol, N. A., & Grin, E. A. (2001). The evolution of lacustrine environments on Mars: Is Mars only hydrologically dormant? *Icarus*, *149*(2), 291–328. https://doi.org/10.1006/icar.2000.6530

Carr, M. H. (1995). The Martian drainage system and the origin of valley networks and fretted channels. *Journal of Geophysical Research*, *100*(E4), 7479–7507. https://doi.org/10.1029/95je00260

Carr, M. H., & Head, J. W. (2003). Oceans on Mars: An assessment of the observational evidence and possible fate. *Journal of Geophysical Research*, *108*(E5), 5042. https://doi.org/10.1029/2002je001963

Christensen, P. R., Jakosky, B., Kieffer, H. H., Malin, M. C., McSween, H. Y., Nealson, K., et al. (2004). The thermal emission imaging system (Themis) for the Mars 2001 Odyssey Mission. *Space Science Reviews*, *110*(1–2), 85–130. https://doi.org/10.1023/b:spac.0000021008.16305.94

Clifford, S. M., & Parker, T. J. (2001). The evolution of the Martian hydrosphere: Implications for the fate of a primordial ocean and the current state of the Northern Plains. *Icarus*, *154*(1), 40–79. https://doi.org/10.1006/icar.2001.6671

Davis, J. M., Balme, M., Grindrod, P. M., Williams, R. M. E., & Gupta, S. (2016). Extensive Noachian fluvial systems in Arabia Terra: Implications for early Martian climate. *Geology*, *44*(10), 847–850. https://doi.org/10.1130/g38247.1

Davis, J. M., Gupta, S., Balme, M., PeterGrindrod, M., Peter, F., I Dickeson, Z., & Williams, R. M. E. (2019). A diverse array of fluvial depositional systems in Arabia Terra: Evidence for mid-Noachian to early Hesperian Rivers on Mars. *Journal of Geophysical Research: Planets*, *124*(7), 1913–1934. https://doi.org/10.1029/2019je005976

Di Achille, G., Gaetano, B. M. H., & Searls, M. L. (2009). Positive identification of lake strandlines in Shalbatana Vallis, Mars. *Geophysical Research Letters*, *36*(14), L14201. https://doi.org/10.1029/2009gl038854

Di Achille, G., & Hynek, B. M. (2010). Ancient Ocean on Mars supported by global distribution of deltas and valleys. *Nature Geoscience*, *3*(7), 459–463. https://doi.org/10.1038/ngeo891

Dickeson, Z. (2022). *Mars palaeolake system - western Arabia Terra - digital elevation models*. FigShare.

Dickeson, Z. I., & Davis, J. M. (2020). Martian oceans. *Astronomy and Geophysics*, *61*(3), 3.11–3.17. https://doi.org/10.1093/astrogeo/ataa038

Dickson, J. L., Lamb, M. P., Williams, R. M. E., Hayden, A. T., & Fischer, W. W. (2020). The global distribution of depositional rivers on early Mars. *Geology*, *49*(5), 504–509. https://doi.org/10.1130/g48457.1

Duran, S., TomCoulthard, J., & Baynes, E. R. C. (2019). Knickpoints in Martian channels indicate past ocean levels. *Scientific Reports*, *9*(1), 1–6. https://doi.org/10.1038/s41598-019-51574-2

Evans, A. J., Andrews-Hanna, J. C., & Zuber, M. T. (2010). Geophysical limitations on the erosion history within Arabia Terra. *115*. E05007. *Journal of Geophysical Research*. https://doi.org/10.1029/2009je003469

Fairén, A. G., Davila, A. F., Lim, D., Nathan, B., Bonaccorsi, R., Zavaleta, J., et al. (2010). Astrobiology through the ages of Mars: The study of terrestrial analogues to understand the habitability of Mars. *Astrobiology*, *10*(8), 821–843. https://doi.org/10.1089/ast.2009.0440

Fassett, C. I., & Goudge, T. A. (2021). Modeling the hydrodynamics, sediment transport, and valley incision of outlet-forming floods from Martian crater lakes. *Journal of Geophysical Research: Planets*, *126*(11), e2021JE006979. https://doi.org/10.1029/2021je006979

Fassett, C. I., & Head, J. W. (2008a). The timing of Martian valley network activity: Constraints from buffered crater counting. *Icarus*, *195*(1), 61–89. https://doi.org/10.1016/j.icarus.2007.12.009

Fassett, C. I., & Head, J. W., III. (2008b). Valley network-fed, open-basin lakes on Mars: Distribution and implications for Noachian surface and subsurface hydrology. *Icarus*, *198*(1), 37–56. https://doi.org/10.1016/j.icarus.2008.06.016

Fassett, C. I., & JamesHead, W., III. (2007). Layered mantling deposits in northeast Arabia Terra, Mars: Noachian-Hesperian sedimentation, erosion, and terrain inversion. *Journal of Geophysical Research*, *112*(E8). https://doi.org/10.1029/2006je002875

Favaro, E. A., Balme, M. R., Davis, J. M., Grindrod, P. M., Fawdon, P., Barrett, A. M., & Lewis, S. R. (2021). The aeolian environment of the landing site for the ExoMars Rosalind Franklin rover in Oxia Planum, Mars. *Journal of Geophysical Research: Planets*, *126*(4), 2020JE006723. https://doi.org/10.1029/2020je006723

Fawdon, P., Balme, M. R., Davis, J. M., Bridges, J. C., Gupta, S., & Quantin-Nataf, C. (2021). Rivers and lakes in Western Arabia Terra: The fluvial catchment of the ExoMars 2022 Rover Landing site. *Journal of Geophysical Research: Planets*, *127*(2), e2021JE007045. https://doi.org/10.1029/2021je007045

Fawdon, P., Gupta, S., JoelDavis, M., Warner, N. H., Adler, J. B., Balme, M. R., et al. (2018). The Hypanis Valles Delta: The last highstand of a sea on early Mars? *Earth and Planetary Science Letters*, *500*, 225–241. https://doi.org/10.1016/j.epsl.2018.07.040

García-Arnay, Á., & Gutiérrez, F. (2020). Reconstructing Paleolakes in Nepenthes Mensae, Mars, using the distribution of putative deltas, coastal-like features, and terrestrial analogs. *Geomorphology*, *359*, 107129. https://doi.org/10.1016/j.geomorph.2020.107129

Goudge, T. A., Aureli, K. L., Head, J. W., CalebFassett, I., & Mustard, J. F. (2015). Classification and analysis of candidate impact crater-hosted closed-basin lakes on Mars. *Icarus*, *260*, 346–367. https://doi.org/10.1016/j.icarus.2015.07.026

Goudge, T. A., CalebFassett, I., & Mohrig, D. (2019). Incision of Paleolake outlet canyons on Mars from overflow flooding. *Geology*, *47*(1), 7–10. https://doi.org/10.1130/g45397.1

Goudge, T. A., & Fassett, C. I. (2018). Incision of Licus Vallis, Mars, from multiple lake overflow floods. *Journal of Geophysical Research-Planets*, *123*(2), 405–420. https://doi.org/10.1002/2017je005438

Goudge, T. A., Fassett, C. I., Head, J. W., Mustard, J. F., & Aureli, K. L. (2016). Insights into surface runoff on early Mars from Paleolake basin morphology and stratigraphy. *Geology*, *44*(6), 419–422. https://doi.org/10.1130/g37734.1

Goudge, T. A., Head, J. W., Mustard, J. F., & CalebFassett, I. (2012). An Analysis of open-basin lake deposits on Mars: Evidence for the nature of associated lacustrine deposits and post-lacustrine modification processes. *Icarus*, *219*(1), 211–229. https://doi.org/10.1016/j.icarus.2012.02.027

Goudge, T. A., Morgan, A. M., Stucky de Quay, G., & Fassett, C. I. (2021). The importance of lake breach floods for valley incision on early Mars. *Nature*, *597*(7878), 645–649. https://doi.org/10.1038/s41586-021-03860-1

Hoke, M. R. T., Hynek, B. M., & Tucker, G. E. (2011). Formation timescales of large Martian valley networks. *Earth and Planetary Science Letters*, *312*(1–2), 1–12. https://doi.org/10.1016/j.epsl.2011.09.053

Howard, A. D., Moore, J. M., & Rossman Irwin, P., III. (2005). An intense terminal epoch of widespread fluvial activity on early Mars: 1. Valley network incision and associated deposits. *Journal of Geophysical Research*, *110*(E12), E12S14. https://doi.org/10.1029/2005je002459

Hynek, B. M., Beach, M., & Hoke, M. R. T. (2010). Updated global map of Martian valley networks and implications for climate and hydrologic processes. *Journal of Geophysical Research*, *115*(Sep), E09008. https://doi.org/10.1029/2009je003548

Irwin, R. P., Rossman, P., Maxwell, T. A., Howard, A. D., Craddock, R. A., & Leverington, D. W. (2002). A large paleolake basin at the head of Ma'adim Vallis, Mars. *Science*, *296*(5576), 2209–2212. https://doi.org/10.1126/science.1071143

Irwin, III, Rossman, P., Howard, A. D., Craddock, R. A., & Moore, J. M. (2005). An intense terminal epoch of widespread fluvial activity on early Mars: 2. Increased runoff and paleolake development. *Journal of Geophysical Research*, *110*(E12), E12S15. https://doi.org/10.1029/2005je002460

Irwin, III, Rossman, P., Howard, A. D., & Maxwell, T. A. (2004). Geomorphology of Ma'adim Vallis, Mars, and associated paleolake basins. *Journal of Geophysical Research*, *109*(E12), E12009. https://doi.org/10.1029/2004je002287

Kirk, R. L., Howington-Kraus, E., Rosiek, M. R., Anderson, J. A., Archinal, B. A., KrisBecker, J., et al. (2008). Ultrahigh resolution topographic mapping of Mars with Mro Hirise stereo images: Meter-scale slopes of candidate phoenix landing sites. *Journal of Geophysical Research*, *113*(E3), E00A24. https://doi.org/10.1029/2007je003000

Kite, E. S. (2019). Geologic constraints on early Mars climate. *Space Science Reviews*, *215*(1), 10. https://doi.org/10.1007/s11214-018-0575-5

Malin, M. C., Bell, J. F., Cantor, B. A., Caplinger, M. A., Calvin, W. M., Clancy, R. T., et al. (2007). Context camera investigation on board the Mars reconnaissance orbiter. *Journal of Geophysical Research*, *112*(E5), E05S04. https://doi.org/10.1029/2006je002808

Mangold, N., & Ansan, V. (2006). Detailed study of an hydrological system of valleys, a delta and lakes in the southwest Thaumasia Region, Mars. *Icarus*, *180*(1), 75–87. https://doi.org/10.1016/j.icarus.2005.08.017

Marra, W. A., Braat, L., Baar, A. W., & Kleinhans, M. G. (2014). Valley formation by groundwater seepage, pressurized groundwater outbursts and crater-lake overflow in flume experiments with implications for Mars. *Icarus*, *232*, 97–117. https://doi.org/10.1016/j.icarus.2013.12.026

McEwen, A. S., Eliason, E. M., Bergstrom, J. W., Bridges, N. T., Hansen, C. J., Delamere, W. A., et al. (2007). Mars reconnaissance orbiter's high resolution imaging science experiment (HiRISE). *Journal of Geophysical Research*, *112*(E5), E05S02. https://doi.org/10.1029/2005je002605

McNeil, J. D., Peter, F., Balme, M. R., & Coe, A. L. (2021). Morphology, morphometry and distribution of isolated landforms in southern Chryse Planitia, Mars. *Journal of Geophysical Research: Planets*, *126*(5), e2020JE006775. https://doi.org/10.1029/2020JE006775

Milliken, R. E., Ewing, R. C., Fischer, W. W., & Hurowitz, J. (2014). Wind-blown sandstones cemented by sulfate and clay minerals in Gale Crater, Mars. *Geophysical Research Letters*, *41*(4), 1149–1154. https://doi.org/10.1002/2013gl059097

Milliken, R. E., Grotzinger, J. P., & Thomson, B. J. (2010). Paleoclimate of Mars as captured by the stratigraphic record in gale crater. *Geophysical Research Letters*, *37*(4). https://doi.org/10.1029/2009gl041870

Neukum, G., & Jaumann, R. (2004). *HRSC: The high resolution stereo camera of mars express* (Vol. 1240). The Scientific Payload.

Parker, T. J., Schneeberger, D. M., Pieri, D. C., & Stephen Saunders, R. (1986). Geomorphic evidence for ancient seas on Mars. *MARS: Evolution of its Climate and Atmosphere*, *599*.

Rivera-Hernández, F., & Palucis, M. C. (2019). Do deltas along the crustal dichotomy boundary of Mars in the gale crater region record a northern ocean? *Geophysical Research Letters*, *46*(15), 8689–8699. https://doi.org/10.1029/2019gl083046

Salese, F., Di Achille, G., Adrian, N., Ori, G. G., & Hauber, E. (2016). Hydrological and sedimentary analyses of well-preserved paleofluvial-paleolacustrine systems at Moa Valles, Mars. *Journal of Geophysical Research: Planets*, *121*(2), 194–232. https://doi.org/10.1002/2015je004891

Salese, F., Kleinhans, M. G., Mangold, N., Ansan, V., McMahon, W., de Haas, T., & Dromart, G. (2020). Estimated minimum life span of the Jezero fluvial delta (Mars). *Astrobiology*, *20*(8), 977–993. https://doi.org/10.1089/ast.2020.2228

Salese, F., Pondrelli, M., Neeseman, A., Schmidt, G., & Ori, G. G. (2019). Geological evidence of planet-wide groundwater system on Mars. *Journal of Geophysical Research: Planets*, *124*(2), 374–395. https://doi.org/10.1029/2018je005802

Sato, H., Kurita, K., & Baratoux, D. (2010). The formation of floor-fractured craters in Xanthe Terra. *Icarus*, *207*(1), 248–264. https://doi.org/10.1016/j.icarus.2009.10.023

Schmidt, G., Luzzi, E., Rossi, A. P., Pondrelli, M., Apuzzo, A., & Salvini, F. (2022). Protracted hydrogeological activity in Arabia Terra, Mars: Evidence from the structure and mineralogy of the layered deposits of Becquerel crater. *Journal of Geophysical Research: Planets*, *127*(9), e2022JE007320. Portico. https://doi.org/10.1029/2022je007320

Schmidt, G., Pondrelli, M., Salese, F., Rossi, A. P., Le Deit, L., Fueten, F., & Salvini, F. (2021). Depositional Controls of the Layered Deposits of Arabia Terra, Mars: Hints From Basin Geometries and Stratigraphic Trends. *Journal of Geophysical Research: Planets*, *126*(11), e2021JE006974. Portico. https://doi.org/10.1029/2021je006974

Smith, D. E., Zuber, M. T., Frey, H. V., Garvin, J. B., Head, J. W., Muhleman, D. O., et al. (2001). Mars orbiter laser altimeter: Experiment summary after the first year of global mapping of Mars. *Journal of Geophysical Research*, *106*(E10), 23689–23722. https://doi.org/10.1029/2000je001364

Tanaka, K. L., Skinner, J. A., Dohm, J. M., Irwin, R. P., Kolb, E. J., Fortezzo, C. M., et al. (2014). *Geologic map of mars, scientific investigations map 3292*. US Geological Survay. https://doi.org/10.3133/sim3292

Tanaka, K. L., Skinner, J. A., Hare, T. M., Joyal, T., & Wenker, A. (2003). Resurfacing history of the northern plains of Mars based on geologic mapping of Mars global surveyor data. *Journal of Geophysical Research*, *108*(E4), 8043. https://doi.org/10.1029/2002je001908

Watters, T. R., PatrickMcGovern, J., & Irwin, R. P., III. (2007). Hemispheres apart: The crustal dichotomy on Mars. *Annual Review of Earth and Planetary Sciences*, *35*(1), 621–652. https://doi.org/10.1146/annurev.earth.35.031306.140220

Webb, V. E. (2004). Putative shorelines in Northern Arabia Terra, Mars. *Journal of Geophysical Research*, *109*(E9), E09010. https://doi.org/10.1029/2003je002205

Williams, R. M. E., Moersch, J. E., & Fergason, R. L. (2018). Thermophysical properties of Martian fluvial sinuous ridges: Inferences on "inverted channel" induration agent. *Earth and Space Science*, *5*(9), 516–528. https://doi.org/10.1029/2018ea000402

Wilson, S. A., Howard, A. D., Moore, J. M., & Grant, J. A. (2016). A cold-wet middle-latitude environment on Mars during the Hesperian-Amazonian transition: Evidence from Northern Arabia Valleys and paleolakes. *Journal of Geophysical Research-Planets*, *121*(9), 1667–1694. https://doi.org/10.1002/2016je005052

Zabrusky, K., Andrews-Hanna, J. C., & Wiseman, S. M. (2012). Reconstructing the distribution and depositional history of the sedimentary deposits of Arabia Terra, Mars. *Icarus*, *220*(2), 311–330. https://doi.org/10.1016/j.icarus.2012.05.007